

High-temperature formation of concentric fullerene-like structures within foam-like carbon: Experiment and molecular dynamics simulation

D. W. M. Lau,¹ D. G. McCulloch,¹ N. A. Marks,² N. R. Madsen,³ and A. V. Rode³

¹*Applied Physics, School of Applied Sciences, RMIT University, GPO Box 2476V, Melbourne, Victoria 3001, Australia*

²*School of Physics, The University of Sydney, New South Wales 2006, Australia*

³*Laser Physics Centre, Research School of Physical Sciences and Engineering, The Australian National University, Canberra, Australian Capital Territory 0200, Australia*

(Received 14 February 2007; revised manuscript received 11 April 2007; published 15 June 2007)

The formation mechanism of carbon onions is investigated. The microstructure of onions formed using pulsed-laser deposition is found to depend critically on the background gas pressure. Molecular dynamics simulations show that an optimal annealing temperature of 4000 K is required to form well-ordered onions (concentric fullerene-like spheres), in agreement with experiment. The onions form from the outer layer first, and a model is presented in which the background pressure must be sufficient to allow atoms to cluster, yet low enough to allow annealing into well-ordered onions.

DOI: [10.1103/PhysRevB.75.233408](https://doi.org/10.1103/PhysRevB.75.233408)

PACS number(s): 61.48.+c, 61.43.Bn, 68.37.Lp, 81.15.Fg

The formation mechanism of carbon onions has remained a mystery ever since they were first observed by Iijima¹ in 1980. Consisting of concentric fullerene-like structures, carbon onions can be formed in a variety of harsh environments such as high energy electron irradiation of a carbon precursor,² thermal annealing of diamond nanoparticles,³ carbon ion implantation,⁴ and arc discharge from a carbon target in water.⁵ Onionlike structures have also been observed in soot⁶ and interstellar dust.⁷ In each case, the formation of onions involves high-temperature heating of carbon precursors, but the nucleation mechanism and range of possible microstructures are poorly understood. Several conceptual models have been proposed for how the onions nucleate and form a three-dimensional structure. For example, Iijima¹ and Ugarte² separately proposed a model in which onions form from a central fullerene seed (e.g., a C₆₀ unit), while Kroto and McKay⁸ proposed a spiral-like growth mechanism.

In this work, we present molecular dynamics (MD) simulations of carbon onion formation and compare our results to experimental observations of material prepared using ultrafast pulsed-laser ablation.⁹ Simulations¹⁰ have proven highly successful in understanding the formation mechanism of fullerenes, which nucleate by the *shrinking hot giant model*, whereby a cluster of atoms form large, closed, caged structures by the aggregation of atoms before shedding chains of *sp*-bonded atoms to form smaller, energetically favorable, fullerene structures. Our simulation procedure is designed to mimic the experimental synthesis of carbon onions from a high-temperature plasma discharge in an inert background gas. The simulations show that multiwalled carbon onions can be formed from a variety of precursors including amorphous carbon and nanodiamond. We find that the key factors which control the carbon onion microstructure are temperature and annealing time. An optimal annealing temperature of 4000 K is observed, and extended annealing in excess of ~ 100 ps is required to access the ordered state. These results are supported by our experimental studies, and explain why onions form in a variety of extreme conditions.

The experiments were conducted in Ar ambient with a graphite target irradiated by a high-repetition-rate Nd:YVO₄

laser operating at 532 nm, generating 12 ps pulses at a repetition rate of 1.5 MHz, with average power 25 W. The laser radiation was focused to a 15 μm diameter spot, producing a laser fluence as high as 10 J/cm². At this laser intensity, the plume of ablated material is fully atomized and partially ionized.¹¹ Several samples were prepared using pressures in the chamber ranging from 2 to 200 Torr. This experimental setup is identical to that used to prepare carbon nanofoams,¹¹ which exhibit unusual para-, superpara-, and ferromagnetic properties.^{12,13} This work reports the characterization of carbon onions which were found within the nanofoam. Samples in the form of powders were collected at a fixed distance of ≈ 5 mm from the target. Figures 1(a)–1(c) show typical transmission electron microscopy (TEM) images of the carbon material. The sample prepared at 50 Torr shows evidence of well-ordered onions containing concentric rings of {002} graphitelike planes. In comparison, the material formed at 200 Torr shows onionlike structures which contain a large number of defects in the graphitic layers. At 2 Torr, the microstructure is more complicated, consisting of small disordered clusters and some fragments of graphitic material.

To determine the density and *sp*² fraction, electron energy loss spectroscopy analysis was performed. For all three samples, the plasmon energy of the $\pi + \sigma$ feature was in the range 21–22 eV. Assuming a free-electron model,¹⁴ these values correspond to local densities of ~ 1.5 – 1.7 g/cc, in contrast with the macroscopic density of the nanofoam which is 3 orders of magnitude lower.¹² The carbon *K* edge was also measured and found to be similar in all cases. The *sp*² fraction was determined to be $\sim 85\%$ using the intensity of the $1s \rightarrow \pi^*$ feature.¹⁵

To evaluate graphitic ordering within a large number of clusters, energy filtered electron diffraction data were collected from an area of each sample. Figure 1(d) shows diffraction profiles as a function of pressure using a radial averaging method described elsewhere.¹⁶ The sample at 50 Torr shows the sharpest {002} peak at $k = 1.77 \text{ \AA}^{-1}$ (where $k = 4\pi/\lambda \sin \theta$) and is similar to commercial glassy carbon heat treated to 2500 K, which shows good in-plane graphitic ordering.¹⁷ At pressures above and below 50 Torr, there is a

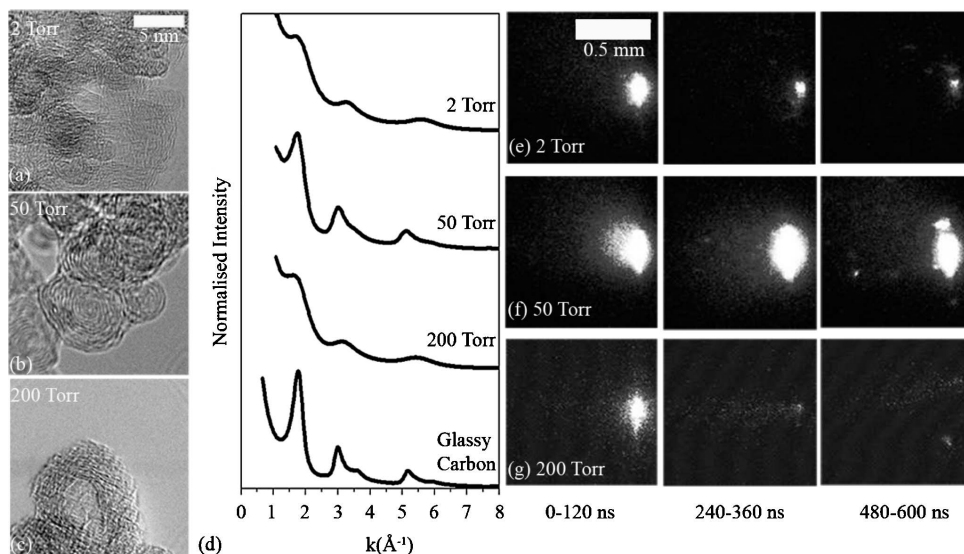


FIG. 1. TEM micrograph of carbon material fabricated with an Ar pressure of (a) 2 Torr, (b) 50 Torr, and (c) 200 Torr. (d) Diffraction intensity profile of the material fabricated at 2, 50, and 200 Torr with the profile for glassy carbon inserted for comparison. (e)–(g) CCD images of the laser plume at various delays and pressures. Each image was integrated for 120 ns over the wavelength range of 220–820 nm.

broadening of the $\{002\}$ peak, indicating less ordering of the graphitic planes.

Insight into the plasma conditions responsible for this behavior is seen in Figs. 1(e)–1(g), which presents charge coupled device (CCD) images of the plasma plume at the beginning, middle, and end of each laser firing cycle. At 1.5 MHz, the period between laser pulses is 667 ns and the images are integrated over the wavelength 220–820 nm within each cycle for a gate width of 120 ns. These measurements show that the plasma plume maintains a high temperature at 50 Torr, which correlates with the optimal conditions for onion formation seen in Figs. 1(a)–1(c).

These observations suggest a formation process for onions in which the Ar pressure plays a critical role.¹¹ Our model is based on the principle of diffusion-limited aggregation, in which the Ar confines the plasma and cools it via argon-carbon collisions. Therefore, at high argon gas pressures, any carbon clusters within the plasma plume will lose temperature rapidly, decreasing the time in which clusters can anneal and, thus, resulting in material with poor graphitic ordering. In contrast, if the amount of argon is low, the mean free path will become comparable to the target/substrate distance and there will be insufficient aggregation of atoms into clusters large enough to form carbon onions. For intermediate Ar pressures, the conditions for onion formation will be optimal due to the combination of agglomeration and sufficient temperature for annealing.

To test these ideas, we investigated the formation of carbon onions with MD simulations using the environment dependent interaction potential (EDIP).¹⁸ EDIP is a bond-order-type empirical potential which describes long-ranged π -repulsion effects, and therefore, is suitable for simulating highly sp^2 systems. Comparison with *ab initio* data shows that EDIP provides an accurate description of bonding in amorphous, liquid, and crystalline carbon.¹⁹ Recent applications include the simulation of thermal spikes²⁰ and temperature effects during thin-film deposition.²¹ Our simulation methodology involves the preparation of a large carbon cluster (many thousands of atoms), which is subsequently annealed for 200 ps (Ref. 22) at temperatures

spanning 2000–6000 K. Simulations were performed in a NVE ensemble, using velocity rescaling thermostats and an integration time step of 0.35 fs. Both amorphous and crystalline clusters were considered, with the former prepared using liquid quenching²³ and periodic boundary conditions. During the annealing cycle, periodic boundary conditions were removed by using a very large supercell. This procedure resulted in a central cluster surrounded by a dilute gas of carbon atoms and fragments. For completeness, we contrast our large-scale methodology with recent tight-binding MD simulations^{24,25} which considered much smaller systems and did not observe onions of the kind reported here.

Figure 2(a) shows a 4096-atom amorphous carbon (*a-C*) precursor generated by liquid quenching at 1.5 g/cc. Annealing at 4000 K drives a dramatic transformation into a carbon onion structure, as seen in side view in Fig. 2(b) and in cross

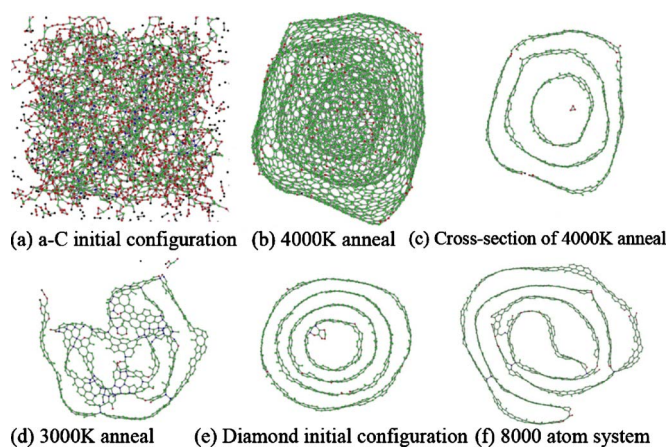


FIG. 2. (Color online) Simulations of carbon onion formation after 200 ps of annealing. (a) 4096-atom amorphous carbon (*a-C*) precursor generated by liquid quenching at 1.5 g/cc. [(b) and (c)] Final structure in plan view and cross section after annealing of the cluster in (a) at 4000 K. (d) Same as (c) but with 3000 K. (e) Same as (c) but with a 4096-atom nanodiamond precursor. (f) Same as (c) but with an 8000-atom *a-C* precursor.

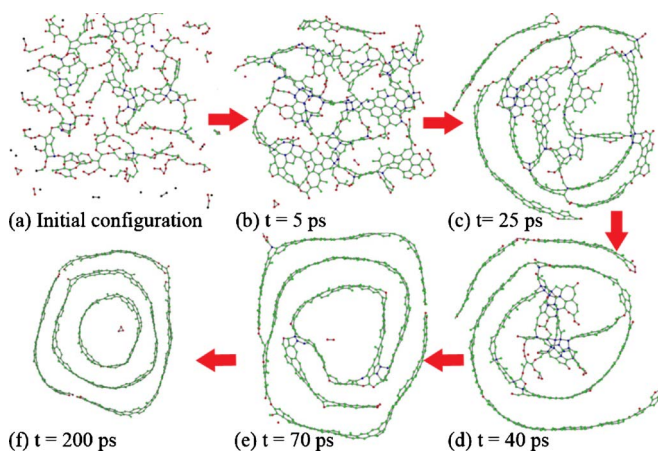


FIG. 3. (Color online) Snapshots showing the formation of the carbon onion seen in Figs. 2(b) and 2(c). Annealing temperature is 4000 K and the annealing time is indicated within each panel.

section in Fig. 2(c). Lower annealing temperatures result in significantly less ordering, as shown by the 3000 K example in Fig. 2(d). Additional simulations using a higher liquid quench density (2.0 and 3.0 g/cc) led to essentially identical final results. This insensitivity to the initial conditions extends to crystalline precursors, as seen in Fig. 2(e) in which a 4096-atom nanodiamond precursor (local density of 3.5 g/cc) similarly transforms into an ordered onion arrangement. While most of our high-temperature simulations led to onionlike structures, in some cases spiral morphologies are observed, as in the 8000-atom simulation of Fig. 2(f).

The temporal evolution of the 4000 K annealed network in Figs. 2(b) and 2(c) is shown in a series of time-lapse cross-sectional snapshots in Fig. 3. Initially, the cluster is devoid of any graphitic ordering, but after 25 ps [Fig. 3(c)] an outer graphitic layer begins to form. At this point, cross-linking between graphite layers is provided by sp^3 -bonded atoms, in a likeness to confluences between graphite planes as proposed for glassy carbon materials.¹⁷ Annealing to 40 ps increases the graphitic layering and a spiral morphology emerges, consistent with the suggestion by Kroto and McKay,⁸ who proposed such a microstructure for carbon onions. However, with further annealing, the structure rearranges, and after 200 ps [Fig. 3(f)], a well-ordered onion is produced with a very high sp^2 fraction of 99%.

The role of temperature during onion formation was studied by a detailed analysis of the 4096-atom 1.5 g/cc a -C precursor. After every picosecond of annealing, a connection list (5 Å cutoff) was constructed to distinguish between (i) atoms still part of the main cluster and (ii) atoms lost into the dilute gas phase. Even with a comparatively low annealing temperature of 2000 K, $\sim 10\%$ of the original atoms are eventually lost. About half of these lost atoms are shed from the initial “cube shape” within the first picosecond, with the remaining eventually boiling away. Similar behavior is observed up to 3500 K, but 4000–4500 K brings the onset of different regimes in which atoms are progressively lost as a function of time. In the most extreme example considered, a simulation at 6000 K lost 73% of atoms after 100 ps, increasing to 93% at 200 ps.

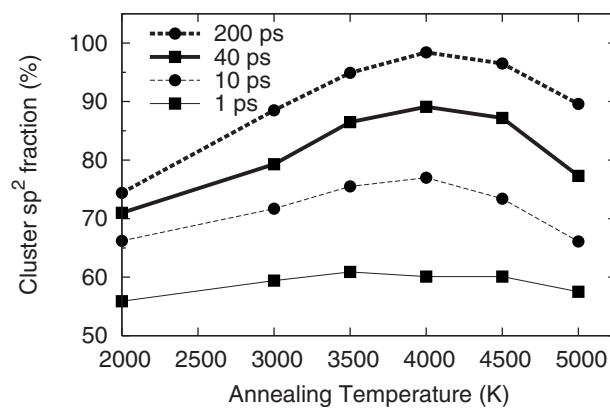


FIG. 4. Proportion of atoms in the central cluster which are sp^2 bonded during annealing of the 1.5 g/cc a -C precursor in Fig. 2(a).

While excessively elevated temperatures preclude onion formation due to material loss, when the annealing temperature is too low the atoms remaining in the cluster are hindered from adopting sp^2 configurations. Figure 4 reveals how low temperatures result in carbon structures which are not particularly onionlike, with 10% sp bonding and 15% sp^3 bonding present in the 2000 K structure after 200 ps. In contrast, annealing at 4000 K results in a structure with 98.4% sp^2 atoms, while at even higher temperatures, sp sites become non-negligible due to temperature-induced mobility. We note that the optimum “temperature window” of 4000 K observed in the simulations correlates closely to two very different experiments involving carbon onions. In the case of ultrafast pulsed-laser deposition in this work, we performed time-resolved optical emission spectroscopy and found that the average temperature in the plasma plume is ~ 4000 K. Similarly, a mathematical analysis of arc discharge by carbon cathodes immersed in water⁵ finds that onions are generated when the carbon atoms have a temperature of approximately 4000 K.

In addition to the suppression of material loss and the promotion of sp^2 bonding, the presence of onionlike structures also requires a high degree of graphitelike ordering. To

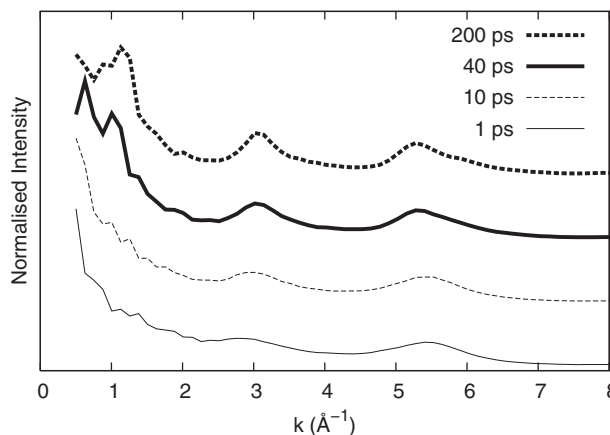


FIG. 5. Diffraction intensity for the 4000 K, 1.5 g/cc simulations as computed using the Debye formula. The amount of ordering as indicated by the $\{002\}$ peak near 1.2 \AA^{-1} increases with annealing time.

characterize this ordering, we applied the Debye formula²⁶ to atoms belonging to the central cluster. These data are presented in Fig. 5, showing the effect of annealing time on graphitic ordering in a cluster at 4000 K. As the annealing time increases, the ordering improves, as shown by the increasing sharpness of the graphitic {002} peak²⁷ at $\sim 1.2 \text{ \AA}^{-1}$. These results support our proposition that clusters which are quenched too rapidly at high argon pressures will contain fewer sp^2 bonds and will have insufficient time to form well-ordered onions. Furthermore, our model is consistent with all of the associated experimental techniques (implantation, irradiation, arc discharge in water, etc.) and illuminates the critical physical phenomena, namely, the delicate balance involving mobility, material loss, intersheet ordering, and sp^2 bonding. These ideas are not dissimilar to recent models pro-

posed for nanotube growth involving solid-phase growth from amorphous carbon precursors.²⁸

In summary, we have investigated the formation of carbon onions in ultrafast laser ablation experiments and in MD simulations. We find that the amount of argon is critical to the formation of well-ordered onions in two ways. First, sufficient argon is required to encourage atoms to cluster and form large enough precursors. Second, the level of argon has to be low enough to allow the carbon precursors to anneal at high enough temperatures long enough to order the precursors into carbon onions. The MD simulations provide atomic-level detail of the formation process, showing that onions form from the outer layer first. The simulations also find that 4000 K is a sweet spot for onion formation, in close agreement with experiments.

-
- ¹S. Iijima, *J. Cryst. Growth* **50**, 675 (1980).
²D. Ugarte, *Nature (London)* **359**, 707 (1992).
³V. L. Kuztensov, A. L. Chuvilin, Y. V. Butenko, I. Y. Mal'kov, and V. M. Titov, *Chem. Phys. Lett.* **222**, 343 (1994).
⁴T. Cabioch, E. Thune, and M. Jaouen, *Phys. Rev. B* **65**, 132103 (2002).
⁵N. Sano, H. Wang, I. Alexandrou, M. Chhowalla, K. B. K. Teo, and G. A. J. Amaratunga, *J. Appl. Phys.* **92**, 2783 (2002).
⁶S. Iijima, T. Wakabayashi, and Y. Achiba, *J. Phys. Chem.* **100**, 5839 (1996).
⁷M. Chhowalla, H. Wang, N. Sano, K. B. K. Teo, S. B. Lee, and G. A. J. Amaratunga, *Phys. Rev. Lett.* **90**, 155504 (2003).
⁸H. W. Kroto and K. McKay, *Nature (London)* **331**, 328 (1988).
⁹E. G. Gamaly, A. V. Rode, and B. Luther-Davies, *J. Appl. Phys.* **85**, 4213 (1999); A. V. Rode, B. Luther-Davies, and E. G. Gamaly, *ibid.* **85**, 4222 (1999).
¹⁰S. Irlé, G. Zheng, Z. Wang, and K. Morokuma, *J. Phys. Chem. B* **110**, 14531 (2006).
¹¹A. V. Rode, E. G. Gamaly, and B. Luther-Davies, *Appl. Phys. A: Mater. Sci. Process.* **70**, 135 (2000).
¹²A. V. Rode *et al.*, *Phys. Rev. B* **70**, 054407 (2004).
¹³D. Arçon, Z. Jagličič, A. Zorko, A. V. Rode, A. G. Christy, N. R. Madsen, E. G. Gamaly, and B. Luther-Davies, *Phys. Rev. B* **74**, 014438 (2006).
¹⁴R. F. Egerton, *Electron Energy-Loss Spectroscopy in the Electron Microscope*, 2nd ed. (Plenum, New York, 1996).
¹⁵S. D. Berger, D. R. McKenzie, and P. J. Martin, *Philos. Mag. Lett.* **57**, 285 (1988).
¹⁶T. C. Petersen, W. McBride, D. G. McCulloch, I. K. Snook, and I. Yarovsky, *Ultramicroscopy* **103**, 275 (2005).
¹⁷G. M. Jenkins and K. Kawamura, *Nature (London)* **231**, 175 (1971).
¹⁸N. A. Marks, *Phys. Rev. B* **63**, 035401 (2001).
¹⁹N. Marks, *J. Phys.: Condens. Matter* **14**, 2901 (2002).
²⁰N. A. Marks, *Diamond Relat. Mater.* **14**, 1223 (2005).
²¹N. A. Marks, M. F. Cover, and C. Kocer, *Appl. Phys. Lett.* **89**, 131924 (2006).
²²The time evolution of the cluster sp^2 fraction was computed, and annealing for 100 ps was found to be insufficient, while the properties of interest reached equilibrium after 200 ps.
²³N. A. Marks, N. C. Cooper, D. R. McKenzie, D. G. McCulloch, P. Bath, and S. P. Russo, *Phys. Rev. B* **65**, 075411 (2002).
²⁴G.-D. Lee, C. Z. Wang, J. Yu, E. Yoon, and K. M. Ho, *Phys. Rev. Lett.* **91**, 265701 (2003).
²⁵M. P. Bogana and L. Colombo, *Appl. Phys. A: Mater. Sci. Process.* **86**, 275 (2007).
²⁶B. E. Warren, *X-Ray Diffraction* (Dover, New York, 1969).
²⁷While EDIP (Ref. 18) contains an accurate description of non-bonded repulsion between graphite planes, for reasons of computational efficiency, it omits the weak long-range van der Waals attraction. As a consequence, the {002} spacing is determined by topological constraints, leading to an overestimate of the inter-shell spacing.
²⁸P. J. F. Harris, *Carbon* **45**, 229 (2007).